

Direct identification of modal parameters using the continuous wavelet transform, case of forced vibration

Safia Bedaoui^{*1,2,3}, Hamid Afra^{4a} and Pierre Argoul^{1b}

¹Laboratoire Navier (ENPC/IFSTTAR/CNRS), Ecole des ponts Paris Tech, Université Paris Est, 6 & 8 Avenue Blaise Pascal, Champs-sur-Marne, 77455 Marne-la-Vallée Cedex 2, France

²Faculty of Civil Engineering, Houari Boumedienne Science & Technology University (USTHB), EL Alia, Bab Ezzouar, Alger, Algeria

³Department of Civil Engineering, Faculty of Engineer Sciences, M'hamed Bougara University, (UMBB), Avenue de l'Indépendance, Boumerdès, Algeria

⁴National Center for Studies and Building Research (CNERIB), cité nouvelle El Mokrani, Souidania, Alger, Algeria

(Received December 30, 2012, Revised October 2, 2013, Accepted January 2, 2014)

Abstract. In this paper, a direct identification of modal parameters using the continuous wavelet transform is proposed. The purpose of this method is to transform the differential equations of motion into a system of algebraic linear equations whose unknown coefficients are modal parameters. The efficiency of the present method is confirmed by numerical data, without and with noise contamination, simulated from a discrete forced system with four degrees-of-freedom (4DOF) proportionally damped.

Keywords: modal identification; dynamics of structures; forced vibration; continuous wavelet transform

1. Introduction

The signal processing by wavelet transform was initially formulated by (Grossmann and Morlet 1984). The wavelet analysis, like all other time-frequency transforms, can identify instantaneous frequencies (time-frequency analysis) and detect discontinuities in signals, long-term evolution (trends), and self-similarity (fractal signals). So, through a better description of the signal, the wavelet analysis facilitates the identification of modal parameters from the vibratory response of mechanical structures. One of the first authors having used the Continuous Wavelet Transform (CWT) for modal identification was Staszewski (Staszewski 1997) in the mid-nineties. He considered the Morlet wavelet function and applied it to estimate the modal damping ratios of a mechanical system. Slavic *et al.* (2003) proposed a closely related method, though their method used the Gabor wavelet function. These identification techniques apply the CWT to the free vibratory response of mechanical systems to identify modal parameters (Le and Argoul 2004). The free response of mechanical systems is usually asymptotic, and in this case the representation of

*Corresponding author, Assistant Professor, E-mail : safibed@yahoo.fr, bedaoui@umbb.dz

^aProfessor, E-mail : afra_hamid@yahoo.com

^bProfessor, E-mail: pierre.argoul@enpc.fr

the CWT is concentrated along a curve in the time-frequency domain, called a “ridge” (Carmona *et al.* 1998). The modal parameters identification can be performed by extracting ridges from the modulus or phase of the CWT of the analyzed signal (Slavic *et al.* 2003, Lardies 2002, Le and Argoul 2004, Argoul and Erlicher 2005, Tan *et al.* 2007, Ülker-Kaustel and Karoumi 2011). A complete procedure for modal identification from free responses based on the CWT is presented by Le and Argoul (Le and Argoul 2004), where the characteristics of three complex mother wavelets are compared: the Morlet wavelet, the Cauchy wavelet and the harmonic wavelet. Chakraborty *et al.* (2006) preferred the modified Littlewood-Paley wavelets because this basis function has the advantage being more closely representative of a vibrating signal. However, this basis function is real and the notion of ridges is more difficult to define in the time-frequency plane. The previous identification techniques are based on the computation of the modulus of the CWT and their efficiency has been tested on free-decay responses of linear structures. Moreover, they have also been applied to the free responses of linear non-proportional damped systems (Erlicher and Argoul 2007), to weakly non-linear systems (Lardies and Ta 2005, Staszewski 1998, Argoul and Le 2003) and to time variant systems (Marchesiello *et al.* 2009), (Kougioumtzoglou and Spanos 2013). These techniques can also be applied to measured responses under ambient vibration by converting random responses to free decay responses with the random decrement technique (Lardies 2002). However, the identification results depend strongly on the accuracy of the random decrement technique, which requires a large number of measurement points.

According to the classification proposed by Maia and al. (Maia *et al.* 1998), the identification methods can be classified as “indirect” or “direct”. In the indirect case, the identification is based on the modal parameters by using the dynamic responses of the structure and these parameters are usually nonlinear in the expression of the dynamic time response, even if the behaviour of the system is linear, which usually leads to the use of an iterative procedure to solve the optimization problem. Convergence problems can then occur, and computational cost becomes high. However, the proposed identification technique can be classified as “direct” because the identification is directly based on the general matrix equation of dynamic equilibrium. As the parameters to be identified are generally linear in the differential equations of motion, which govern the dynamical behaviour of the system, direct methods use linear operators to the set of differential equations of motion, transforming them into an algebraic system. This leads to classical linear optimization that can be solved in one step by singular value decomposition or normal equations. Orthogonal functions are frequently used because of their property of integration, based on a square matrix with constant elements. This property allows for the transformation of the set of differential equations, which govern the dynamical behaviour of the system, into a set of algebraic equations. Several methods have already been proposed to transform differential equations governing mechanical system behaviour into algebraic equations by using the well-known properties of polynomial functions. They are called Continuous Time Identification (CTI) methods within the field of systems theory (Mensler 1999). In CTI approaches, orthogonal functions are frequently used for the integral formulation of differential equations (Mensler 1999, Pacheco and Steffen 2002, Rémond *et al.* 2008). Their main advantage is that they transform the integration of signals into a simpler integration of these functions by using a square matrix that depends on the orthogonal functions. Therefore, the differential equations governing the behaviour of the mechanical discrete system can be transformed into algebraic equations. Pacheco and Steffen (2002) compared different kinds of orthogonal bases such as Jacobi, Legendre or Chebyshev polynomials, Block-Pulse or Walsh functions and, of course, Fourier series. They also mentioned the case of integral formulation in the field of inverse problems and the simplicity of calculation

for sensitivity analysis problems.

More recently, Rémond *et al.* (2008) used Chebyshev polynomials to improve classical CTI methods for the identification and inverse formulation of mechanical systems. To avoid some problems with these polynomials, they proposed alternative formulations to first decompose the signal into components and then to estimate the parameters for each component of the signal. Rouby *et al.* (2010) proposed a unified formulation of a direct identification method for linear mechanical systems. Linear operators are applied to the set of motion differential equations, transforming it into an algebraic system. The cases of expansion on Chebyshev polynomials and of Cauchy CWT are studied with a focus on their similarities and differences in writing and performances. Here, in the same way, the CWT is applied directly to the differential equations that govern the dynamic behaviour of the studied discrete system. However, the modal matrix is first identified from the extracted ridges of the transient part of the responses and then applied to transform the motion equations in a simpler form, that are decoupled in the case of proportional damping.

The result is a set of algebraic equations where the unknowns are the mechanical parameters to be identified. The number of identified parameters is far less than the number of algebraic equations. Usually, the algebraic equations are linear with respect to the modal parameters to be identified. A simple linear regression technique can then give an estimation of the parameters. The proposed methodology is then validated by numerically simulated responses from discrete systems.

As mentioned previously, the aim of this paper is to propose a direct identification of modal parameters using the continuous wavelet transform. Firstly, the CWT method is presented as well as its characteristics useful for our study. In the second step, the identification of modal parameters, obtained by solving the differential equation of motion, is illustrated in the case of the forced vibrations of a linear oscillator. Finally, the proposed method is presented in more detail and applied to the case of the forced vibrations of a mechanical linear system with multiple Degrees of Freedom (DoF).

2. The Continuous Cauchy Wavelet Transform (CCWT)

The CWT of a real signal $u(t)$ of finite energy is defined by (Mallat 1999):

$$T_{\psi}[u(t)](b, a) = \frac{1}{a} \int_{-\infty}^{+\infty} u(t) \bar{\psi}\left(\frac{t-b}{a}\right) dt \quad (1)$$

Where the analyzing function $\psi(t)$ is called the “mother wavelet” and $\bar{\psi}(t)$ is its complex conjugate. The real parameters a ($a > 0$) and b introduce scale-dilation and time-translation, respectively and the CWT makes use of shifted and scaled copies of $\psi(t)$: $\psi_{b,a}(t) = \frac{1}{a} \psi\left(\frac{t-b}{a}\right)$ whose $L(R)$ norms are independent of a . An alternative formulation of the wavelet transform can be obtained by applying Parseval’s theorem to Eq. (1):

$$T_{\psi}[u](b, a) = \langle u(t), \psi_{(b,a)}(t) \rangle = \frac{1}{2\pi} \int_{-\infty}^{+\infty} \hat{u}(\omega) \bar{\hat{\psi}}(a\omega) e^{i\omega b} d\omega \quad (2)$$

Where $\hat{\psi}(\omega) = \int_{-\infty}^{+\infty} \psi(t) e^{-i\omega t} dt$ is the Fourier transform of the mother wavelet. In the time-frequency plot, the squared modulus of the CWT represents the signal energy density and is called the scalogram:

$$SCAL_u^{(\psi)}(b, f) = \left| T_\psi[u(t)]\left(b, \frac{f_0}{f}\right) \right|^2 \quad (3)$$

where $f_0 = 2\pi\omega_0$ is the angular frequency when the absolute value of the Fourier transform $\hat{\psi}(\omega)$ of the mother wavelet exhibits a peak. The normalized scalogram defines a local wavelet spectrum:

$$E_{u,CWT}(b, f) = \frac{1}{4\pi C_\psi f} \left| T_\psi[u]\left(b, \frac{f_0}{f}\right) \right|^2, \text{ which has been widely used for the analysis of}$$

non-stationary signals (Carmona *et al.* 1998) and also for the analysis of structure responses under ambient excitations (Argoul *et al.* 2005).

In the case of a frequency and amplitude modulated signal with M distinct frequency components, defined as: $u(t) = \sum_{j=1}^M u_j(t) = \sum_{j=1}^M A_j(t) \cos(\alpha_j(t))$ where the variation of the

amplitude $A_j(t)$ is slow compared to that of the phase $\alpha_j(t)$ (asymptotic signals), the scalogram of the signal $u(t)$ has one particularity : there exists a set of special points in the time-scale plane (b, a) called ridges, such that the energy of the CWT of $u(t)$ tends to be localized around each ridge, and this restriction of the CWT to all ridges, called the ‘‘skeleton’’, is very close to the signal itself. There are several ways to define a ridge (for more details see (Carmona *et al.* 1998)); we used the one where the ridge corresponds to the region where the modulus of the CWT is maximum:

$$R_j^{(u)} = \left\{ (b, a_{r_j}^{(u)}(b)) \mid a_{r_j}^{(u)}(b) = \frac{\omega_0}{\dot{\alpha}_j^{(u)}(b)} \right\} \quad (4)$$

Where $a_{r_j}^{(u)}(b)$ is the scale parameter corresponding to the j^{th} ridge present in the CWT of the signal. Extracting the ridge and calculating the skeleton allow for an estimation of the frequency content of the signal and its reconstruction. Eq. (5) states that the CWT of an asymptotic signal u_j computed on the ridge is proportional to the complex signal $z^{(u_j)}(b)$:

$$T_\psi[u_j](b, a_{r_j}^{(u_j)}(b)) \approx T_\psi[u](b, a_{r_j}^{(u)}(b)) = \frac{1}{2} \hat{\psi}(\omega_0) z^{(u_j)}(b) \quad (5)$$

With $z^{(u_j)}(b)$ being the analytic signal associated with the component u_j (for more details see (Carmona *et al.* 1998, Argoul and Le 2003)). The following Eq. (6) shows that it is possible to isolate the j^{th} frequency component $u_j(b)$ from the CWT of a multi-component signal:

$$u_j(b) = \text{Re}\{z^{(u_j)}(b)\} \approx \text{Re}\left\{ \frac{2T_\psi[u](b, a_{r_j}^{(u)}(b))}{\hat{\psi}(\omega_0)} \right\} \quad (6)$$

where $\text{Re}\{\}$ is the real part of the complex function within brackets.

In our study, we used the standard Cauchy wavelet $\psi_n(t)$ with order n obtained from the modified Cauchy wavelet: $\psi_n(t) = \left(\frac{i}{\beta t + i} \right)^{n+1}$ with $\beta = 1$. In the following, ψ is replaced by ψ_n and the CWT becomes the Continuous Cauchy Wavelet Transform (CCWT). The uncertainty of ψ_n is: $\mu_{\psi_n} = \frac{1}{2} \sqrt{\frac{2n+1}{2n-1}}$ (Erlicher and Argoul 2007). The Heisenberg uncertainty principle states that the uncertainty is always greater than or equal to 1/2 (Carmona *et al.* 1998). For the Cauchy wavelet, as n is increasing, the value of μ_{ψ_n} rapidly becomes close to the boundary 0.5: $\mu_{\psi_{10}} = 0.53$, $\mu_{\psi_{50}} = 0.510$, $\mu_{\psi_{100}} = 0.505$, etc.

The Fourier transform of ψ_n is: $\hat{\psi}_n(\omega) = (2\pi\omega^n e^{-\omega} / n!) H(\omega)$ where $H(\omega)$ is the Heaviside function. Cauchy wavelets and their first and second derivatives are admissible and progressive (Le and Argoul 2004); for instance, the wavelet is progressive when: $\hat{\psi}_n(\omega) = 0: \forall \omega \leq 0$. Using integration by parts and due to the properties for the decrease of the functions $\psi_n(t)$ when $|t| \rightarrow +\infty$, we obtain:

$$T_{\psi_n} [\dot{u}(t)](b, a) = -\frac{1}{a} T_{\dot{\psi}_n} [u(t)](b, a) = -\frac{i(n+1)}{a} T_{\psi_{n+1}} [u(t)](b, a) \quad (7)$$

$$T_{\psi_n} [\ddot{u}(t)](b, a) = \frac{1}{a^2} T_{\ddot{\psi}_n} [u(t)](b, a) = -\frac{(n+1)(n+2)}{a^2} T_{\psi_{n+2}} [u(t)](b, a) \quad (8)$$

The choice of the Cauchy mother wavelet ψ_n is crucial in Eqs. (7) and (8) because its first and second derivatives are directly linked to Cauchy mother wavelets of higher order: $\dot{\psi}_n(t) = i(n+1)\psi_{n+1}(t)$ and $\ddot{\psi}_n(t) = -(n+1)(n+2)\psi_{n+2}(t)$. Thus, the CCWT of order n of the first derivative of a signal can be related to the CCWT of order $n+1$ of the signal. This property is not retained for the modified Morlet mother wavelet used by several authors (for example (Lardies 2002): $\psi_{\omega_0, N}(t) = e^{i\omega_0 t} e^{-\frac{t^2}{M}}$ ($M > 0$) whose first derivation $\dot{\psi}_{\omega_0, N}(t) = \psi_{\omega_0, N}(t)(i\omega_0 - 2\frac{t}{M})$ is no longer a Morlet wavelet. In (Le and Argoul 2004), the authors, referring to the frequency analysis filters, compared the wavelet analysis to a band pass filter with a quality factor Q defined as:

$$Q = \frac{\omega}{2\Delta\omega} = \frac{\omega_\psi / a}{2(\Delta\omega_\psi / a)} = \frac{\omega_{\psi_{b,a}}}{2\Delta\omega_{\psi_{b,a}}} \quad (9)$$

and equal to $Q = \frac{\sqrt{2n+1}}{2}$ for the standard Cauchy wavelet ψ_n . Moreover, to avoid modal coupling and the problem of edge effects, the values for the quality factor are chosen as follows:

$$Q_{\min} \leq Q \leq Q_{\max} \quad \text{with} \quad Q_{\min} = c_f \frac{\omega_j}{2d\omega_j} \quad \text{and} \quad Q_{\max} = \frac{L\omega_j}{4c_t \mu_\psi} \quad \text{where} \quad c_f \quad \text{and} \quad c_t \quad \text{are coefficients}$$

whose values are close to 5, L is the finite length of the recorded signal, ω_j is the frequency to identify for $1 \leq j \leq M$, and $d\omega_j = \min((\omega_j - \omega_{j-1}), (\omega_{j+1} - \omega_j))$ is a characteristic angular frequency discrepancy between two close angular frequencies with $\omega_0 = 0$ and $\omega_{M+1} = \frac{\pi}{L}$. The choice of a suitable c_f value, i.e. a value such that the residual edge effects do not affect the modal identification substantially, has already been discussed in (Erlicher and Argoul 2007) without making reference to a specific mother wavelet. In the following, we choose: $c_f = c_f = 5$.

3. Identification method

In this part, we introduce the direct modal parameter identification method by applying the CCWT to the differential motion equations. Two types of linear systems will be studied: an oscillator with viscous damping and a discrete system with N DoF assuming proportional viscous damping.

3.1 Case of a linear oscillator with viscous damping

Here, we are studying the case of a linear oscillator with an angular frequency ω , damping factor ξ and mass m . This oscillator is subjected to an excitation $p(t)$ applied to the mass m . Setting $\alpha = \omega^2$, and $\beta = 2\xi\omega$ with $\alpha > 0$, $\beta > 0$ and $\alpha > \frac{\beta^2}{4}$, the normalized differential equation of motion is written as follows:

$$\ddot{u}(t) + \beta\dot{u}(t) + \alpha u(t) = \frac{1}{m} p(t) \quad (10)$$

$$u(0) = u_0 \quad (11)$$

$$\dot{u}(0) = \dot{u}_0 \quad (12)$$

where $u(t)$ is the displacement of the mass m , and u_0 and \dot{u}_0 are the initial conditions. The response $u(t)$ can be written as the sum of the transient part and the steady state part: $u(t) = u^{(tr)}(t) + u^{(st)}(t)$ which satisfy respectively:

$$\ddot{u}^{(tr)}(t) + \beta\dot{u}^{(tr)}(t) + \alpha u^{(tr)}(t) = 0 \quad (13)$$

$$\ddot{u}^{(st)}(t) + \beta\dot{u}^{(st)}(t) + \alpha u^{(st)}(t) = \frac{1}{m} p(t) \quad (14)$$

The general expression of the transient part $u^{(tr)}$ and of the steady state part are given by:

$$u^{(tr)} = e^{-\frac{\beta}{2}t} \left(u_0 \cos \tilde{\omega}t + \frac{1}{\tilde{\omega}} (\dot{u}_0 + \beta u_0 \sin \tilde{\omega}t) \right) \quad (15)$$

and

$$u^{st}(t) = \int_0^t \frac{1}{m} p(\tau) h(t-\tau) d\tau \tag{16}$$

Where $h(t)$ is the impulse response function: $h(t) = \frac{1}{m\tilde{\omega}} e^{-\frac{\beta}{2}t} \sin \tilde{\omega}t$ with $\tilde{\omega} = \sqrt{\alpha - \frac{\beta^2}{4}}$. As the CCWT is a linear operator, we apply the CCWT to the previous Eqs. (13) and (14) with the mother wavelet and we obtain:

$$T_{\psi_n} [\ddot{u}^{(tr)}(t)](b, a) + \beta T_{\psi_n} [u^{(tr)}(t)](b, a) + \alpha T_{\psi_n} [u^{(tr)}(t)](b, a) = 0 \tag{17}$$

$$T_{\psi_n} [\ddot{u}^{(st)}(t)](b, a) + \beta T_{\psi_n} [u^{(st)}(t)](b, a) + \alpha T_{\psi_n} [u^{(st)}(t)](b, a) = \frac{1}{m} T_{\psi_n} [p(t)](b, a) \tag{18}$$

Both of these equations must hold for all pairs (b, a) . When the ridge of the CCWT of $u^{(tr)}$ is far enough from one of the ridges of the CCWT of $u^{(st)}$: $R^{u^{(tr)}} \cap R^{u^{(st)}} = \emptyset$, there are two interesting sets of points: points on the ridge of the CCWT of $u^{(tr)}$: $a = a_r^{u^{(tr)}}$, where $T_{\psi_n} [u^{(tr)}](b, a_r^{u^{(tr)}}(b)) \approx T_{\psi_n} [u](b, a_r^{u^{(tr)}}(b))$ and points on the ridge of the CCWT of $u^{(st)}$: $a = a_r^{u^{(st)}}$ (b), where $T_{\psi_n} [u^{(st)}](b, a_r^{u^{(st)}}(b)) \approx T_{\psi_n} [u](b, a_r^{u^{(st)}}(b))$.

For the first case: $a = a_r^{u^{(tr)}}$, Eq. (17) can be rewritten as:

$$T_{\psi_n} [\ddot{u}^{(tr)}(t)](b, a_r^{u^{(tr)}}(b)) + \beta T_{\psi_n} [u^{(tr)}(t)](b, a_r^{u^{(tr)}}(b)) + \alpha T_{\psi_n} [u^{(tr)}(t)](b, a_r^{u^{(tr)}}(b)) = 0 \tag{19}$$

and for the second case: $a = a_r^{u^{(st)}}(b)$, Eq. (18) can be rewritten as:

$$T_{\psi_n} [\ddot{u}^{(st)}(t)](b, a_r^{u^{(st)}}(b)) + \beta T_{\psi_n} [u^{(st)}(t)](b, a_r^{u^{(st)}}(b)) + \alpha T_{\psi_n} [u^{(st)}(t)](b, a_r^{u^{(st)}}(b)) = \frac{1}{m} T_{\psi_n} [p(t)](b, a_r^{u^{(st)}}(b)) \tag{20}$$

By substituting Eqs. (7) and (8) into the two previous Eqs. (19) and (20), we obtain:

$$\frac{-(n+1)(n+2)}{(a_r^{u^{(tr)}})^2} T_{\psi_{n+2}} [u](b, a_r^{u^{(tr)}}(b)) - i \frac{\beta(n+1)}{a_r^{u^{(tr)}}} T_{\psi_{n+1}} [u](b, a_r^{u^{(tr)}}(b)) + \alpha T_{\psi_n} [u](b, a_r^{u^{(tr)}}(b)) = 0 \tag{21}$$

$$\frac{-(n'+1)(n'+2)}{(a_r^{u^{(st)}})^2} T_{\psi_{n'+2}} [u](b, a_r^{u^{(st)}}(b)) - i \frac{\beta(n'+1)}{a_r^{u^{(st)}}} T_{\psi_{n'+1}} [u](b, a_r^{u^{(st)}}(b)) \tag{22}$$

$$+ \alpha T_{\psi_n} [u](b, a_r^{u^{(st)}}(b)) = \frac{1}{m} T_{\psi_n} [p](b, a_r^{u^{(st)}}(b))$$

By setting: $W_m(b, a) = \frac{(m+1)(m+2)}{a^2} T_{\psi_{m+2}} [u](b, a)$, $U_m(b, a) = -\frac{(m+1)}{a} T_{\psi_{m+1}} [u](b, a)$, $S_m(b, a) = T_{\psi_m} [u](b, a)$ and $Y_m(b, a) = T_{\psi_m} [p](b, a)$, and after separating the real and imaginary parts of Eqs.

(21) and (22), we obtain the system of equations below:

$$\begin{cases} \alpha \operatorname{Re}\left\{S_n\left(b, a_r^{u^{(tr)}}(b)\right)\right\} - \beta \operatorname{Im}\left\{U_n\left(b, a_r^{u^{(tr)}}(b)\right)\right\} & = \operatorname{Re}\left\{W_n\left(b, a_r^{u^{(tr)}}(b)\right)\right\} \\ \alpha \operatorname{Im}\left\{S_n\left(b, a_r^{u^{(tr)}}(b)\right)\right\} - \beta \operatorname{Re}\left\{U_n\left(b, a_r^{u^{(tr)}}(b)\right)\right\} & = \operatorname{Im}\left\{W_n\left(b, a_r^{u^{(tr)}}(b)\right)\right\} \\ \alpha \operatorname{Re}\left\{S_n\left(b, a_r^{u^{(st)}}(b)\right)\right\} - \beta \operatorname{Im}\left\{U_n\left(b, a_r^{u^{(st)}}(b)\right)\right\} - \frac{1}{m} \operatorname{Re}\left\{Y_n\left(b, a_r^{u^{(st)}}(b)\right)\right\} & = \operatorname{Re}\left\{W_n\left(b, a_r^{u^{(st)}}(b)\right)\right\} \\ \alpha \operatorname{Im}\left\{S_n\left(b, a_r^{u^{(st)}}(b)\right)\right\} - \beta \operatorname{Re}\left\{U_n\left(b, a_r^{u^{(st)}}(b)\right)\right\} - \frac{1}{m} \operatorname{Im}\left\{Y_n\left(b, a_r^{u^{(st)}}(b)\right)\right\} & = \operatorname{Im}\left\{W_n\left(b, a_r^{u^{(st)}}(b)\right)\right\} \end{cases} \quad (23)$$

The three parameters α , β and m to be identified are solutions of the algebraic system of Eq. (23) which can be written for any point $(b, a_r^{u^{(tr)}})$ on the ridge of $u^{(tr)}$ for the two first equations and for any point $(b, a_r^{u^{(st)}})$ on the ridge of $u^{(st)}$ for the two last equations. For all the points on both ridges, we obtain a system of algebraic equations with three unknowns (α , β and $1/m$) that can be written in matrix form: $A\underline{x} = \underline{y}$. This equation is solved by MATLAB software with the normal equation: $x = (A^T A)^{-1} A^T y$, assuming $A^T A$ invertible; this resolves the problem of inversion by minimizing $\|A\underline{x} - \underline{y}\|^2$ in the least squares sense.

In the case of a linear oscillator submitted to an external force, three parameters α , β and $1/m$ are to be identified. Two points, at least, of the time-frequency plane are needed: one on the ridge of the transient response and one on the steady-state response. However, the efficiency of the proposed identification technique depends strongly on the location and the number of points chosen along the ridge under consideration. They must be chosen in the time-frequency plane where edge effects are negligible. For example, when ω is the modal angular frequency under consideration, b will belong to $[t', t'']$ where the interval $[t', t'']$ is included in the validity domain of the CCWT so that: $[t', t''] \subset \left[\frac{c_t Q 2 \mu_\psi}{\omega_2}, L - \frac{c_t Q 2 \mu_\psi}{\omega_1} \right]$, ω_1 and ω_2 being close to ω

(Le and Argoul 2004). In our study, the ridges are extracted by using the Crazy Climber's Algorithm (CCA) (Carmona *et al.* 1998). In the CCA, a number of particles (the climbers) are initially randomly seeded on a domain D in the time-frequency plane at initial step. Then each climber starts a random walk on D influenced (in a way similar to the simulated annealing algorithm) by the local values of the scalogram $SCAL_u^{(\psi)}(b, f)$ of the measured signal u . In summary, the algorithm combines simulated annealing in the frequency f direction and symmetric random walk in the time b direction (Carmona *et al.* 1999).

3.2 Case of a linear proportionally damped system with multiple DoF

In this part, we are interested by the case of linear system with N DoF, using proportional damping (also called Basile's hypothesis in French terminology). During the tests, N_p measurement points are collected with $N_p \leq N$. So, by using the principle of mode superposition, the k^{th} component ($1 \leq k \leq N_p$) of the displacement vector is given by: $u_k(t) = \sum_{j=1}^N u_{kj}(t) = \sum_{j=1}^N \varphi_{kj} q_j(t)$

where $q_j(t)$ is the generalized modal coordinate of the j^{th} mode and φ_{kj} is the component (k, j) of the modal matrix Φ that has dimensions $(N \times N)$. The columns of Φ are formed by the N real modal

shapes: $\underline{\varphi}_j = \{\varphi_{1j}, \varphi_{2j}, \dots, \varphi_{Nj}\}^T$ for $1 \leq j \leq N$, having orthogonal properties according to the mass matrix \mathbf{M} , stiffness matrix \mathbf{K} , and damping matrix \mathbf{C} . Each modal shape has to be normalized; we chose $\varphi_{ij} = 1$ for all $j \in [1, N]$.

By applying Basile's hypothesis (or Rayleigh's hypothesis of proportionality between stiffness and damping), we have: $\underline{\phi}_i^T \mathbf{M} \underline{\phi}_j = m_i \delta_{ij}$, $\underline{\phi}_i^T \mathbf{K} \underline{\phi}_j = k_i \delta_{ij}$ and $\underline{\phi}_i^T \mathbf{C} \underline{\phi}_j = c_i \delta_{ij} = 2 m_i \omega_i \delta_{ij}$. Setting $\alpha_j = \omega_j^2$ and $\beta_j = 2 \zeta_j \omega_j$ and we can express the N decoupled differential equations of motion as follows: $\ddot{q}_j(t) + \beta_j \dot{q}_j(t) + \alpha_j q_j(t) = \frac{1}{m_j} p_j(t)$.

Two initial conditions must be imposed: $q_j(0) = q_{j,0}$ and $\dot{q}(0) = \dot{q}_{j,0}$

As in the case of single degree of freedom, the generalized response $q_j(t)$ for the j^{th} mode is the sum of the transient and steady state parts: $q_j(t) = q_j^{(tr)}(t) + q_j^{(st)}(t)$ where:

$$q_j^{(tr)}(t) = e^{-\frac{\beta_j}{2}t} \left(q_{j,0} \cos \tilde{\omega}_j t + \frac{1}{\tilde{\omega}_j} (\dot{q}_{j,0} + \beta_j q_{j,0}) \sin \tilde{\omega}_j t \right) \tag{24}$$

and

$$q_j^{(st)}(t) = \frac{1}{m_j} \int_0^t p_j(\tau) h_j(t - \tau) d\tau \tag{25}$$

where $h_j(t)$ is the j^{th} impulse response function: $h_j(t) = \frac{1}{m_j \tilde{\omega}_j} e^{-\frac{\beta_j}{2}t} \sin \tilde{\omega}_j t$ with $\tilde{\omega}_j = \sqrt{\alpha_j - \frac{\beta_j^2}{4}}$.

For the generalized response $q_j(t)$, the identification process of the three parameters α_j , β_j and m_j would be the same as in the case of a simple oscillator. However, $u_k(t) = \sum_{j=1}^N \varphi_{kj} q_j(t)$ is measured instead of $q_j(t)$. The linearity property of CCWT allows to write:

$$\begin{aligned} T_{\psi_n} [u_k](b, a) &= T_{\psi_n} \left[\sum_{j=1}^N u_{kj}(t) \right] (b, a) = \sum_{j=1}^N T_{\psi_n} [u_{kj}(t)] (b, a) \\ &= \sum_{j=1}^N \varphi_{kj} (T_{\psi_n} [q_j^{(tr)}(t)] (b, a) + T_{\psi_n} [q_j^{(st)}(t)] (b, a)) \end{aligned} \tag{26}$$

but knowledge of the CCWT of $q_j^{(tr)}$ or of $q_j^{(st)}$ needs the assessment of the modal matrix.

Thus, the first step is the identification of the modal matrix Φ from the transient part. From the expression of the modal components $u_{kj}^{(tr)}(t)$, it can be easily deduced that:

$$\frac{u_{kj}^{(tr)}(t)}{u_{1j}^{(tr)}(t)} = \frac{\varphi_{kj} q_j(t)}{\varphi_{1j} q_j(t)} = \varphi_{kj} \tag{27}$$

From Eq. (6), it is possible to isolate the j^{th} frequency component $u_{kj}^{(tr)}(b)$ of $u_k(b)$ from the CCWT of the multi-component signal $u_k(b)$.

$$u_k^{(tr)}(b) \approx \text{Re} \left\{ \frac{2T_{\psi_n} [u_k] (b, a_{r_j}^{(tr)}(b))}{\bar{\psi}_n(\omega_0)} \right\} \quad (28)$$

and similarly with the j^{th} frequency component $u_{ij}^{(tr)}(b)$ of $u_i(b)$.

$$u_{ij}^{(tr)}(b) \approx \text{Re} \left\{ \frac{2T_{\psi_n} [u_i] (b, a_{r_j}^{(tr)}(b))}{\bar{\psi}_n(\omega_0)} \right\} \quad (29)$$

Finally, we obtain:

$$\phi_{kj} \approx \frac{\text{Re} \left\{ T_{\psi_n} [u_k(t)] (b, a_{r_j}^{(tr)}(b)) \right\}}{\text{Re} \left\{ T_{\psi} [u_i(t)] (b, a_{r_j}^{(tr)}(b)) \right\}} \quad (30)$$

From the j^{th} extracted ridges R_{kj} extracted from the transient part of each response u_k , the relationship Eq. (30) allows to estimate ϕ_{kj} by computing the following parameter:

$$\phi_{kj} \approx \frac{\sum_{l=1}^{N_{R_j}} \frac{\text{Re} \left\{ T_{\psi_n} [u_k(t)] (b, a_{r_j}^{(tr)}(b_l)) \right\}}{\text{Re} \left\{ T_{\psi} [u_i(t)] (b, a_{r_j}^{(tr)}(b_l)) \right\}}}{N_{R_j}} \quad (31)$$

computed with N_{R_j} points chosen on the ridge R_j of the time interval previously defined to

avoid edge effects: $b_l \in \left[\frac{c_l Q 2 \mu_{\psi}}{\omega_j}, L - \frac{c_l Q 2 \mu_{\psi}}{\omega_j} \right]$.

Then, it will be possible to calculate the generalized response vector: $\underline{q} = \Phi^{-1} \underline{u}$.

Finally, in the same way as in the case of a single DoF system, the modal parameters : β_j , α_j and m_j can be estimated for each mode j .

The procedure to identify the modal parameters for N DoF system, is given below:

- Compute and plot the scalogram signals of vector \underline{u} with the curves of side-effects, which limit the validity domain.
- Extract the ridges by applying the CCA.
- Estimate the modal matrix from the transient part of each measured signal.
- For each mode, resolve Eq. (23) as in the case of a linear oscillator.

4. Application to a system with four DoF

4.1 Numerical response without noise

The Fig. 1 illustrates the 4 DoF system used for testing the efficiency of our method. Its exact modal frequencies f_j for $1 \leq j \leq 4$ and the corresponding quality factors are given in Table 1.

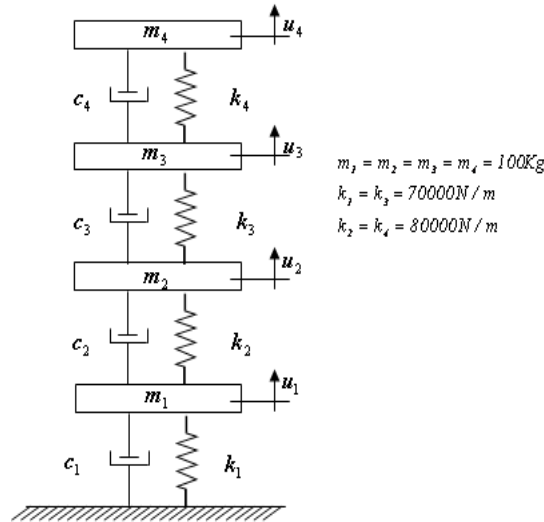


Fig. 1 (4DoF) system with proportional damping

Table 1 Values of the exact frequencies and quality factor Q_j for each mode

Frequency band [Hz]	Exact frequency f_j [Hz]	Interval of the Quality factor	Quality factor Q_j
$0.02 \leq f \leq 2.92$	1.499	$3.54 < Q < 15.04$	10
$2.92 \leq f \leq 5.56$	4.298	$4.56 < Q < 42.60$	30
$5.56 \leq f \leq 7.52$	6.800	$15.59 < Q < 67.26$	40
$7.52 \leq f \leq 10.0$	8.203	$15.95 < Q < 81.44$	45

This system is then subjected to a harmonic force: $F(t) = F_0 \sin(\omega_F t)$ with $\omega_F = 2\pi f_F = 2\pi 12 = 75.40 \text{ rds}^{-1}$ and to an initial displacement of: $u_1(0) = u_2(0) = u_3(0) = u_4(0) = 10^{-3} \text{ m}$.

For each mode of vibration, the CCWT is computed for a frequency band centered around its eigen frequency f_j and for an adapted quality factor Q_j for $1 \leq j \leq 4$. The quality factors for extracting each modal component j are chosen to satisfy the inequality: $Q_{\min} \leq Q_j \leq Q_{\max}$ in order to avoid edge effects and modal coupling as presented before. Finally, the quality factor for the extraction of the harmonic excitation force is taken equal to 50.

Exact and identified modal parameters (eigen frequencies f_j , modal damping ratio ζ_j and modal mass m_j) for each mode are given in Table 2 as well as the relative errors between the exact values and the identified ones. These errors are very small (around 1%), demonstrating the effectiveness of the method in identifying modal parameters in the case of a linear model with proportional viscous damping.

The Fig. 2(a) shows the time evolution of the first component $u_1(t)$ of the displacement. Its Fourier spectrum is given in Fig. 2(b), and its scalogram with extracted ridges in Fig. 2(c), where the four green curves represent each of the four ridges associated to the transient part $u_{ij}^{(tr)}(t)$ of each modal component $u_{ij}(t)$ ($1 \leq j \leq 4$) of $u_1(t)$. The yellow curve corresponds to the ridge of the steady state part $u_1^{(st)}(t)$ of $u_1(t)$. In Fig. 2(c), the bounds of the time interval chosen for the

Table 2 Exact and identified modal parameters, without noise

Mode	Damping			Frequency			Modal mass		
	exact value [%]	identified value [%]	relative error [%]	exact value [Hz]	identified value [Hz]	relative error [%]	exact value [Kg]	identified value [Kg]	relative error [%]
1	2.00	1.98	0.98	1.499	1.499	0.00	1731.00	1731.38	0.02
2	2.00	1.97	1.45	4.298	4.300	0.05	278.50	281.21	0.97
3	2.67	2.65	0.86	6.800	6.800	0.00	262.86	263.05	0.07
4	3.10	3.07	1.17	8.203	8.202	0.01	493.26	500.67	1.50

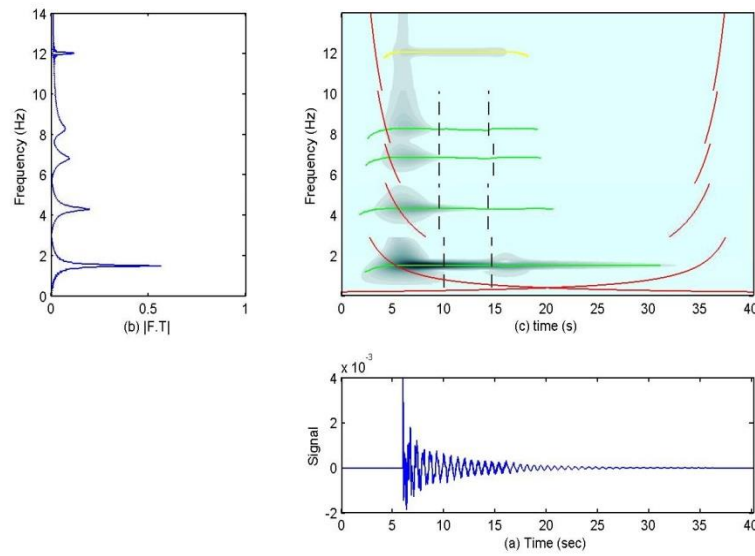


Fig. 2 (4 DoF) system : (a) time representation of $u_i(t)$, (b) its fourier spectrum and (c) its scalogram and extracted ridges

identification along each ridge are also indicated with two black dotted lines.

Due to the edge effect and in order to well illustrate the vibration responses in the time-frequency domain, we used the zero padding technique by adding zeros to time-domain signal for $0 \leq t \leq 6$ and $34 \leq t \leq 40$ s, see Fig. 2(a).

The identified components φ_{ij} of the normalized modal matrix are compared to the exact ones in Table 3. It can be noted that the discrepancies between the exact and identified values are very small and, this proves the effectiveness of the proposed method.

4.2 Analysis of noise effects

To test the influence of noise effects on the results of the proposed identification method, an amount of noise $\eta_k(t)$ is added to the simulated signals $u_k(t)$. It is modeled by the centered normal distribution. This noise representation is classically used with simulated data as large frequency

bandwidth components in order to analyse the robustness of the method. The signal-to-noise ratio (*SNR*):

$$SNR^{(u_k)} = 10 \text{Log} \frac{\text{Variance}(u_k(t))}{\text{Variance}(\eta_k(t))} \quad (32)$$

is then used in order to compare the level of the signal to the level of noise. Two cases corresponding to $SNR^{(u_k)} = 19.22 \text{dB}$ (strong noise) and $SNR^{(u_k)} = 63.81 \text{dB}$ (weak noise) are considered. Figs. 3 and 4 present the time and the frequency evolutions, as well as the scalogram of $u_i(t)$ when perturbed by a noise with a *SNR* of 19.22dB and 63.81dB , respectively. The identification results given in Tables 3, 4 and 5, show that the proposed method is quite effective, even in presence of noise.

Table 3 Exact and identified modal shapes

Modal Shapes	Exact Values	Identified modal shapes		
		Without noise	Noise of 63dB	Noise of 19dB
ϕ_{11}	1	1	1	1
ϕ_{12}	1.764	1.764	1.765	1.760
ϕ_{13}	2.414	2.414	2.417	2.419
ϕ_{14}	2.715	2.715	2.718	2.730
ϕ_{21}	1	1	1	1
ϕ_{22}	0.964	0.964	0.964	0.965
ϕ_{23}	-0.082	-0.082	-0.076	-0.090
ϕ_{24}	0.922	-0.923	-0.917	-0.935
ϕ_{31}	1	1	1	1
ϕ_{32}	-0.407	-0.405	-0.401	-0.395
ϕ_{33}	-0.954	-0.955	-0.950	-0.901
ϕ_{34}	0.744	0.744	0.745	0.741
ϕ_{41}	1	1	1	1
ϕ_{42}	-1.446	-1.417	-1.331	-1.410
ϕ_{43}	1.246	1.239	1.173	1.247
ϕ_{44}	-0.537	-0.550	-0.580	-0.579

Table 4 Exact and identified modal parameters, weak noise - $SNR=63.81 \text{dB}$

Mode	Damping			Frequency			Modal mass		
	exact value [%]	identified value [%]	relative error [%]	Exact value [Hz]	identified value [Hz]	relative error [%]	exact value [Kg]	identified value [Kg]	relative error [%]
1	2.00	2.02	1.22	1.499	1.499	0.00	1731.00	1716.22	0.85
2	2.00	1.86	7.03	4.298	4.250	1.10	278.50	280.49	0.59
3	2.67	2.65	0.76	6.800	6.817	0.26	262.86	264.93	0.79
4	3.10	3.07	1.15	8.203	8.202	0.01	493.26	523.63	6.15

Table 5 Exact and identified modal parameters, strong noise $-SNR=19.22dB$

Mode	Damping			Frequency			Modal mass		
	exact value [%]	identified value [%]	relative error [%]	exact value [Hz]	identified value [Hz]	relative error [%]	exact value [Kg]	identified value [Kg]	relative error [%]
1	2.00	2.00	0.20	1.499	1.499	0.00	1731.00	1891.52	9.27
2	2.00	1.55	22.35	4.298	4.246	1.20	278.50	285.68	2.37
3	2.67	2.79	4.43	6.800	6.804	0.06	262.86	262.68	0.07
4	3.10	2.75	11.39	8.203	8.198	0.06	493.26	513.24	4.05

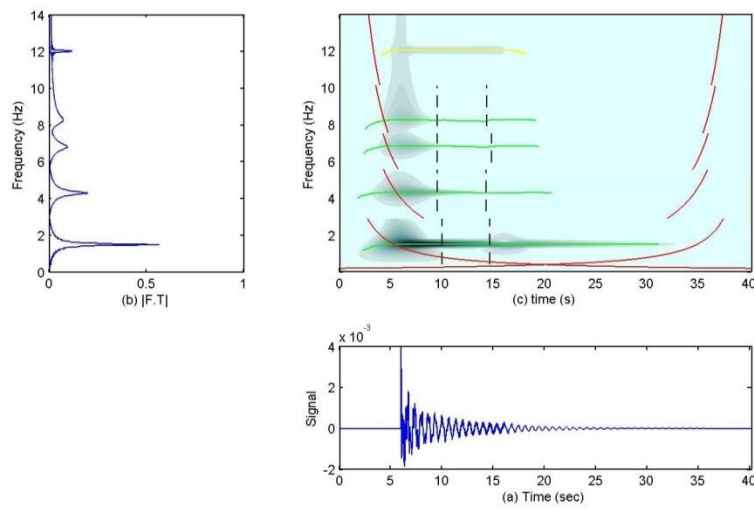


Fig. 3 (4Dof) system – case of noise : $SNR=63.81dB$ - (a) time representation of $u_1(t)$, (b) its fourier spectrum and (c) its scalogram and extracted ridges

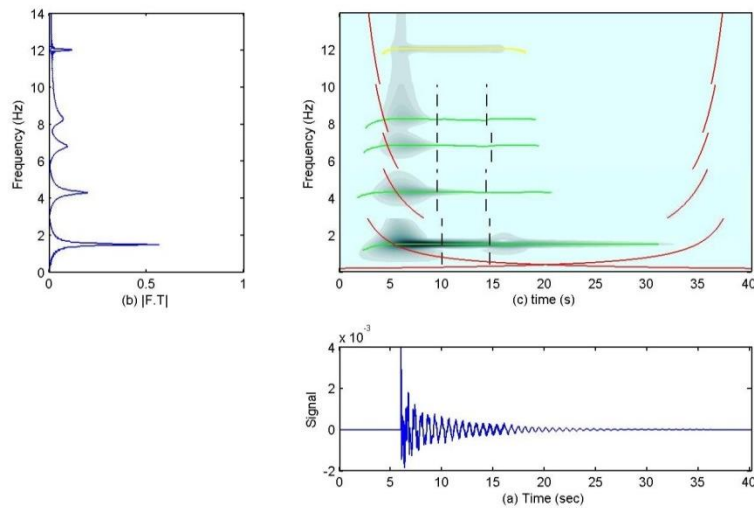


Fig. 4 (4Dof) system – case of strong noise : $SNR=19.22dB$ - (a) Time representation of $u_1(t)$, (b) its Fourier spectrum and (c) its scalogram and extracted ridges

5. Conclusions

In this paper, a direct parameter identification method based on the continuous wavelet transform is presented. This method is applied to forced responses of linear structures and their modal parameters are identified. Its efficiency has been tested on numerical simulations. The effect of additive white noise on signals is also investigated. The identification results are very satisfactory even in the presence of noisy signals. Its application to other real cases of civil engineering structures is under study.

Acknowledgments

The authors are indebted to Didier Rémond for their useful and interesting discussions about this work. They would also like to thank Maria Aristova and Tiffany Hwang of Princeton University for their help editing this article.

References

- Argoul, P. and Erlicher, S. (2005), "On the use of continuous wavelet analysis for modal identification", *Mechanical Modelling and Computational Issues in Civil Engineering, Lecture Notes in Applied and Computational Mechanics*, Volume 23, 359-368.
- Argoul, P., Erlicher, S. and Nguyen, T.M. (2005), "Free oscillations of a beam with a local non-linearity: comparison of mechanical modeling and experiments by means of wavelet analysis", *ASME International Design Engineering Technical Conferences and Computers and Information in Engineering Conferences*, Long Beach, California, USA, 24th- 28th September.
- Argoul, P. and Le, T.P. (2003), "Instantaneous indicators of structural behaviour based on continuous Cauchy wavelet transform", *Mech. Syst. Signal Pr.*, **17**(1), 243-250.
- Carmona, R., Hwang, W.L. and Torr sani, B. (1998), *Practical time-frequency analysis*, Academic Press, New York, USA.
- Carmona, R., Hwang, W.L. and Torr sani, B. (1999), "Multiridge detection and time-frequency reconstructions", *IEEE T. Signal Proces.*, **47**(2), 480-492.
- Chakraborty, A., Basua, B. and Mitra, M. (2006), "Identification of modal parameters of a mdof system by modified Littlewood-Paley wavelet packets", *J. Sound Vib.*, **295**(3-5), 827-837.
- Erlicher, S. and Argoul, P. (2007), "Modal identification of linear non-proportionally damped systems by wavelet transform", *Mech. Syst. Signal Pr.*, **21**(3), 1386-1421.
- Grossmann, A. and Morlet, J. (1984), "Decomposition of hardy functions into square integrable wavelets of constant shapes", *SIAM J. Math. Anal.*, **15**(4), 723-736.
- Kougioumtzoglou, I.A. and Spanos, P.D. (2013), "An identification approach for linear and nonlinear time-variant structural via harmonic wavelet", *Mech. Syst. Signal Pr.*, **37**(1-2), 338-352.
- Lardies, J. (2002), "Identification of modal parameters using the wavelet transform", *Int. J. Mech. Sci.*, **44**(11), 2263-2283.
- Lardies, J. and Ta, M.N. (2005), "A wavelet based approach for the identification of damping in non-linear oscillators", *Int. J. Mech. Sci.*, **47**(8), 1262-1281.
- Le, T.P. and Argoul, P. (2004), "Continuous wavelet transform for modal identification using free decay response", *J. Sound Vib.*, **277**(1-2), 73-100.
- Maia, N.M.M., Silva, J.M.M., He, N.J., Lieven, N.A.J., Lin, R.M., Skingle, G.W., To, W.M. and Urgueira, A.P.V. (1998), *Theoretical and experimental modal analysis*, Research Studies Press Ltd., Hertfordshire, England.

- Mallat, S. (1999), *A wavelet tour of signal processing*, Elsevier Academic Press, Sang Diego.
- Marchesiello, S., Bedaoui, S., Garibaldi, L. and Argoul, P. (2009), "Time-dependent identification of a bridge-like structure with crossing loads", *Mech. Syst. Signal Pr.*, **23**(6), 2019-2028.
- Mensler, M. (1999), "Analyse et étude comparative de méthodes d'identification des systèmes à représentation continue : développement d'une boîte à outils logicielle Université Henri Poincaré"—Nancy, France. ("Analysis and comparative study of continuous-time system identification techniques. Development of the CONTSID toolbox", PhD thesis, Henri Poincaré University, Nancy 1, French)
- Pacheco, R.P. and Steffen, V.Jr. (2002), "Using orthogonal functions for identification and sensitivity analysis of mechanical systems", *J. Vib. Control*, **8**(7), 993-1021.
- Rémond, D., Neyrand, J., Aridon, G. and Dufour, R. (2008), "On the improved use of Chebyshev expansion for mechanical system identification", *Mech. Syst. Signal Pr.*, **22**(2), 390-407.
- Rouby, C., Rémond, D. and Argoul, P. (2010), "Orthogonal polynomials or wavelet analysis for mechanical system direct identification", *Ann. Solid Struct. Mech.*, **1**(1), 41-58.
- Slavic, J., Simonovski, I. and Boltezar, M. (2003), "Damping identification using a continuous wavelet transform: application to real data", *J. Sound Vib.*, **262**(2), 291-307.
- Staszewski, W.J. (1997), "Identification of damping in MDof systems using time-scale decomposition", *J. Sound Vib.*, **203**(2), 283-305.
- Staszewski, W.J. (1998), "Identification of nonlinear systems using multi-scale ridges and skeletons of the wavelet transform", *J. Sound Vib.*, **214**(4), 639-658.
- Tan, J.B., Liu, Y., Wang, L. and Yang, W.G. (2007), "Identification of modal parameters of a system with high damping and closely spaced modes by combining continuous wavelet transform with pattern search", *Mech. Syst. Signal Pr.*, **22**(5), 1055-1060.
- Ülker-Kaustell, M. and Karoumi, R. (2011), "Application of the continuous wavelet transform on the free vibration of a steel-concrete composite railway bridge", *Eng. Struct.*, **33**(3), 911-919.